Microsyst Technol (2016) 22:1915–1926
DOI 10.1007/s00542-016-2890-7

TECHNICAL PAPER

Non-invasive voltage measurement in a three-phase autonomous meter

Davide Brunelli[1] · Clemente Villani[2] · Domenico Balsamo[2] · Luca Benini[2,3]

Received: 31 August 2015 / Accepted: 22 February 2016 / Published online: 12 April 2016
© Springer-Verlag Berlin Heidelberg 2016

Abstract Monitoring current and voltage waveforms is essential to evaluate the energy consumption of a system and to improve its efficiency. In this paper we present a smart meter for power consumption which can measure both current and voltage without any physical contact to the electric load or to the conductors of the power cables. This makes the power metering much safer and easier; furthermore an energy harvesting module based on inductive coupling provides power supply to the meter without any need of batteries or plugs to the mains. We describe the innovative contact-less voltage measurement system, which is based on capacitive coupling and uses an algorithm with two pre-processing channels for self-calibration and to provide accurate measurements regardless the cable type. The three-phase version is capable of measuring the three-phase power consumption of an electric load in a complete contact-less manner. In comparison with commercial high-cost instruments, experimental results of our low-cost smart meter demonstrate similar high performance with maximum 3 % deviation from the reference value.

1 Introduction

Nowadays the electric energy demand is constantly increasing, and while the primary energy resources are decreasing, the exploitation of renewable energy sources is not yet widespread enough to cope with the growing need of electrical energy (Waeresch et al. 2015). Electrical energy management is becoming crucial to optimize the way to produce, to distribute and to use energy. Today, Smart Grids integrate ICT capability into the power grid to enhance the efficiency, reliability, economics, and sustainability of the production and distribution of electricity (Amin and Wollenberg 2005) and forecasting of the consumption (Quilumba et al. 2015). Among the services delivered by Smart Grids, intelligent, unobtrusive and unattended energy metering is key to profile the quality and the quantity of the energy delivered and to detect failures. Furthermore, energy metering offers a wide range of applications oriented to consumers, such as real time energy monitoring systems used to track and analyze the power consumption of industrial loads. In this way, users can reduce energy waste (Ahmad 2011) and the electrical bill, as well. For this purpose, low-cost, meters, will play an increasingly important role (Depuru et al. 2011; Campbell and Dutta 2014) in the future, in particular if massively deployed to monitor in a pervasive way the electric power consumed correlated to everyday activities. The procedures of installation of these measurement systems do not facilitate today the widespread diffusion of such energy meters, because they are usually not inexpensive and they need expert technicians to connect the meters to the mains.

For a pervasive exploitation, power meters should use non-intrusive sensors, which can easily be installed in any circumstances by any user without disconnection of the electrical loads; with a small form factor, and should operate unattended for years.

In this paper, we present an electrical energy meter which meets all the above user requirements and can be extended even for three-phase measurements. The meter

✉ Davide Brunelli
davide.brunelli@unitn.it

[1] DII, University of Trento, via Sommarive 9, Trento 38123, Italy

[2] DEI, University of Bologna, viale Risorgimento 2, Bologna, Italy

[3] IIS, ETHZ, Gloriastrasse 35, Zurich, Switzerland

is energy autonomous, namely it harvest energy from the environment to reduce costs of battery replacement, and analyzes voltage and current waveforms with power quality estimation without any direct contact to the conductors of the power cables. Hence, our smart meter permits the implementation of non-intrusive load monitoring (NILM) techniques for disaggregating global energy consumption data in a household scenario (Liang et al. 2010a, b).

The meter exploits a clamp-on sensor for both current measurement and energy harvesting, and new voltage contact-less sensors, based on capacitive coupling, that permits to measure the difference of electrical potential between two conductors in a single-phase power line. Our goal is to obtain an easy-to-install device which does not need any interruption of the 230 V AC power supply, and can be installed without any interruption of the loads. The voltage measurement front-end can self-calibrate to sense current and voltage waveforms regardless of the size and the type of the cable. Although the smart sensor node is non-intrusive and low-cost, its metric performance is comparable to the results obtained with professional expensive and intrusive measurement instruments. Finally, we present the three-phase version of the device designed to measure current and voltage waveforms from three-phase AC power systems.

The paper is organized as follows. Section 2 presents an overview of the non-intrusive measurement systems. In Sect. 3, we describe in detail the proposed smart sensor node, with a focus on the designed non-intrusive voltage measurement system. The design of the three-phase front-end extension is discussed in Sect. 4, while Sect. 5 shows the experimental results. Finally, Sect. 6 concludes the paper.

2 Related works

The measurement of current is a well-established technique, using either magnetic transducers or shunt resistors. Shunt resistors are a widespread and inexpensive method which however suffers of an error on accuracy higher than 5 % (Misti et al. 2014) and necessitate of particular designs because the non-galvanic isolation between the acquisition system and the load. For this reason, the measurement through the magnetic field across a single wire is preferable and plenty of transducers such as Rogowsky coils, current transformers or Hall effect sensors (Ripka 2010; Ziegler et al. 2009; Xiao 2003) are available on the market. A survey of smart electricity meters and their utilization, highlighting challenges as well as opportunities arising due to the advent of big data is reviewed in (Alahakoon and Yu 2016).

For voltage measurement, to the best of our knowledge, there is no commercially available non-invasive sensor that can measure the voltage in wires for single-phase or three-phase lines (usually 230–380–400 VAC). Some solutions proposed in literature focus on monitoring in extra/high-voltage (EHV/HV) power systems. For example, the authors in (Wu et al. 2011) present a method to measure the voltage based on a capacitive system, but the monitored voltages are of the order of hundreds of kV. HV Metering has demonstrated that customer voltage measurements exhibit hierarchical correlations which are consistent with the hierarchical connectivity relationships that exist between customers and distribution network (Mitra et al. 2015). The authors in (Kubo et al. 2009) propose a new resin-molded sensor for voltage and current monitoring, which measures power consumption, power factor and harmonics in 6.6 kV power line systems.

However, solutions developed for high voltage (HV) monitoring are usually designed for a different purpose because they are mainly exploited to gather information on overvoltage events and fast transient voltage waveforms, which could create problems on the HV management. They basically probe the time derivative of the phase voltages and the waveform can be restored either by numerical integration or by an analog integrator as part of the measuring system. This integration create drifts in the estimation of the continuous voltage monitoring which is hard to eliminate. In summary, the HV solutions are mainly designed to detect abrupt events and not for a continuous and regular acquisition of the waveform. Moreover HV capacitive sensors are usually not selective for a single-phase voltage, while it is a main requirement which has driven our work.

Recently some solutions for 230 V AC voltage power system have been proposed, but none of them is suitable for our purpose. For example, in (Tsang and Chan 2011) a sensor with two capacitive probes for 230 V AC systems is used to monitor the voltage on a conductor without making direct contact with it. However, the proposed sensor is conceived to be used in voltage monitoring of conductors with planar surfaces, as opposed to most common cylindrical conductors, such as wires or cables. Finally, the authors in (Chen et al. 2014) present a single sensor capable of measuring both the current and the voltage on a type of cable for domestic applications, but, for the particular materials and production processes used to realize it, the cost is remarkably high, and, most of all, the sensor is suitable for only one type of cables. Recently, the combination between hardware front-end and signal processing has been pushed further in (Borkowski et al. 2015), where voltage waveforms are reconstructed by artificial neural network (ANN) using the signals originating from electric field sensors. The system under measurement is yet another medium voltage (MV) substation, where costs and safety

requirements still justifies complex and expensive solutions like this. Data gathered from meters have been used also in (Waeresch et al. 2015; Alimardani et al. 2015) where algorithms for linear LV state estimation are developed based on smart meter data. The approach uses a relatively high measurement redundancy, which is not common for state estimation in LV grids, and which are given by new generation metering systems.

In this paper we propose a non-invasive method for measuring the 230 V AC voltage waveform (low voltage (LV) configuration) between the wires of a single-phase or three-phase power line. The proposed approach does not require interruption of power supply, which makes measurements much safer and easy, and includes an algorithm for self-calibrating which permit the measure regardless the type and the size of the cables typical in residential and industrial buildings.

3 System description

In this section we present the enhancements to the wireless meter presented in (Porcarelli et al. 2013; Balsamo et al. 2013; Villani et al. 2015) to obtain a complete non-intrusive and self-powered meter, capable of sensing in a contactless manner. Moreover, the proposed extensions of the ADC front-end permit the usage both for a single-phase and for a three-phase electrical load regardless the type of cable. The firmware on board elaborates the current waveform and calculates some power quality features of the electric load such as power factor, apparent power, active power and reactive power. The block diagram of the proposed smart meter is shown in Fig. 1.

The contactless voltage and current sensors are connected to the energy harvesting system (that supplies the whole node) and to the analog front end, that pre-processes the signals. The microcontroller computes the measurement data and send it to the local central gateway through the wireless module. Each meter exploits from one to three clamp-on transformers used for both current measurement and energy harvesting. The non-invasive capacitive-coupling sensors for voltage measurement are also used for each cable.

In the following subsections, we describe the four main design blocks of the meter architecture: (1) the microcontroller and wireless transceiver, (2) the current sensing section, (3) the energy harvester, (4) the voltage sensing section.

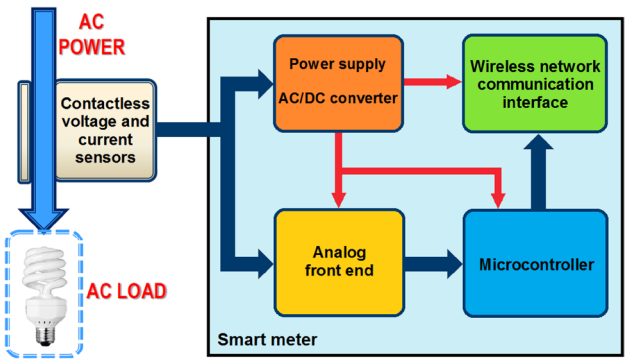

Fig. 1 Block diagram of the proposed smart meter

3.1 Microcontroller and wireless transceiver

The smart meter architecture is based on the JN5148 module from NXP, which provides an ultra-low power, high performance wireless microcontroller targeted to WSN applications, a 512 kB serial flash memory and a real-time clock. The microcontroller features an enhanced 32-bit RISC processor, a 2.4 GHz IEEE 802.15.4 compliant radio transceiver, 128 kB ROM, 128 kB RAM, and a complete set of analogue and digital peripherals such as a 12-bit ADC, a 12-bit DAC, a SPI interface etc. The key features of the JN5148 module are the very low sleep current, only 2.6 μA, and the low power consumption of the radio transceiver (namely at 3.0 V it draws 15 mA during transmission and 17.5 mA when receiving).

The smart meter transmits data to the Energy@Home compliant Gateway (Alahakoon et al. 2016) (connected to a java-enabled host), using ZigBee PRO protocol with Home Automation profile. This gateway is a commercial product called FlexKey[1] and it is one of the most compact Zigbee USB Dongle available on the market today. Due to its RF performance, it enables secure and reliable wireless connectivity between internal and external environment.

3.2 Current sensing section

To assess the current we used a clamp-on current transformer, which can be easily wrapped around the cable, thus it does not require any interruption of the load or any wire cuts for series insertion. The installation is therefore much easier and safer to install. The adopted current transformer features linear performance over a wide range of input currents. Its main electrical characteristics are the number of turns ($n = 3000$) and the maximum input current of 60A for the cable under measurement (primary), which corresponds to a maximum output current from the secondary winding of 20 mA. Figure 2 shows the schematic view of the current measurement circuit.

[1] http://www.flexgrid.it/eng/prodotti/flexkey.html.

The current coming from the inductive coupling is switched (with a relay controlled by the MCU) between the energy harvesting system and the current measurement circuit, where it is converted, with a resistance, to a proportional voltage, which is then sampled by the MCU internal ADC and elaborated by the 32-bit microcontroller.

3.3 Energy harvester

The energy harvesting circuit exploits the same current transformer used for the current measurement as power transducer, with the switching system shown in Fig. 2. When the node is in sleep mode, the energy harvesting unit charges the supercapacitor used as energy buffer. Since the acquisition of each samples from the ADC takes few milliseconds, the remaining time is used for energy harvesting, which leverages the measurement's duty-cycle for recovering the energy spent in measurement mode, in which the transformer is used for sensing current. Using the supercapacitor, the smart meter performs a start-up without any external energy storage (such as a battery). Figure 3 shows the schematic view of the energy harvesting system. The system starts executing the association with the gateway only when the supercapacitor has collected enough energy for completing the network joining. This is guaranteed by the use of an ultra-low power voltage monitor (Vcc monitor) which enable the power supply to the whole wireless meter only when the energy reservoir passes a preset voltage level, which means that the energy stored in the supercapacitor suffices for the start-up completion.

The AC to DC converter is a full-wave passive rectifier, realized by four Schottky diodes with very low forward voltage to minimize power losses across the bridge. The energy buffer is a 1F electric double layer capacitor with 2.5 mΩ internal resistance. An external battery is connected only during the MCU programming. An over-voltage protection circuit and a Vcc monitor circuit keep Vcc stable within a ±10 % at the nominal value of 3.3 V.

3.4 Voltage sensing section

The knowledge of the voltage waveform is important for measuring the Power Factor (PF), that is the ratio between the real power P (measured in W) and the apparent power |S| (measured in VA, where S is the complex power, measured in VA and given by the sum of active power P and reactive power Q, measured in var). PF spans from 0 to 1, but international regulations suggest to keep it bigger than

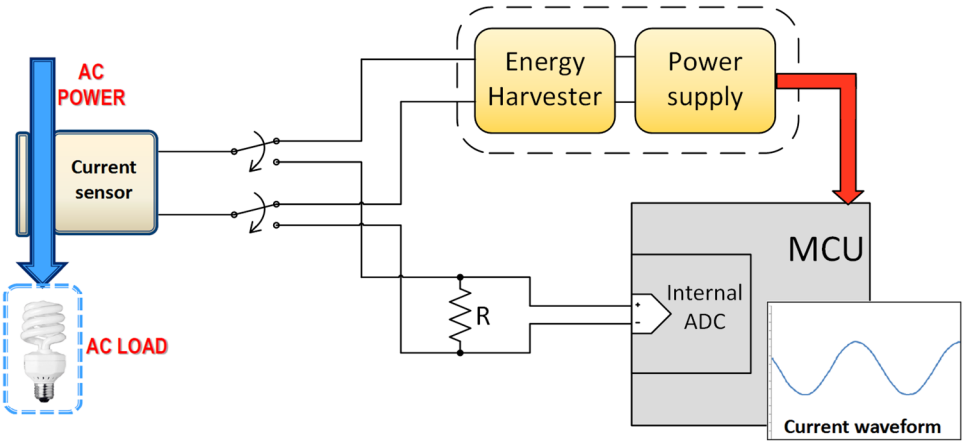

Fig. 2 Schematic view of the current sensing section, where the current sensor output is switched between the energy harvesting system and the current measurement circuit

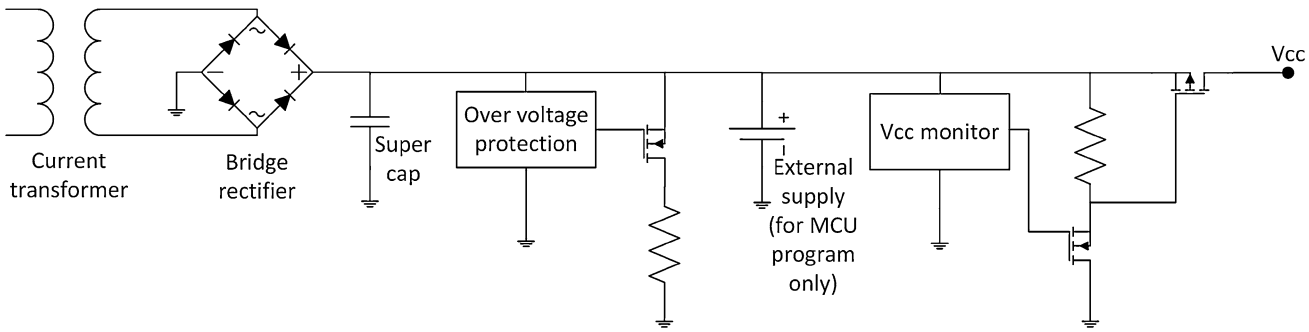

Fig. 3 Schematic view of the energy harvesting system

Fig. 4 **a** Scheme of the capacitance-coupling voltage sensor. **b** Photo of the sensor

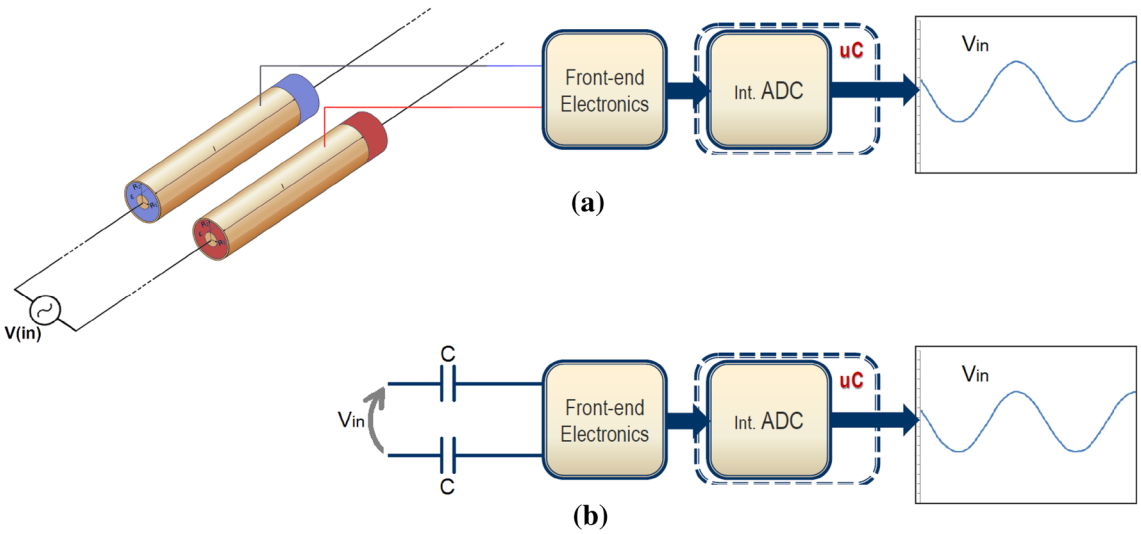

Fig. 5 **a** Block diagram of the voltage measurement system. **b** Equivalent circuit for the analog front-end input

0.9 using dedicated compensation circuits. It is important to note that the PF value measures not just the contribution of the phase lag ϕ between voltage and current, but also the high frequency content of the input current. This harmonic content, as well as the phase lag ϕ, is regulated by the European Standard EN 60555, which defines the limits and the constraints for appliances and mains.

In the following subsections, we present the innovative non-intrusive and self-calibrating system we designed for electrical potential difference measurement.

3.5 Voltage sensors

The voltage sensors is based on capacitive coupling: we put a cylindrical conductor of length l = 1.25 cm around the cable, as shown in Fig. 4.

In this way, we obtain a cylindrical capacitor consisting in the internal conductor of the wire, of radius R1, and the external hollow conductor, of radius R2, separated by the insulating of the cable, with permittivity ε. The capacitance between the two conductors of such structure is given by the formula:

$$C = \frac{2\pi l \varepsilon}{\ln \frac{R_1}{R_2}} \tag{1}$$

Considering a normal cable for domestic applications, with $R_1 = 2 \div 3$ mm, $R_2 = 3 \div 4$ mm, and a PVC insulator, C is in the order of pF, as evaluated from the Eq. (1).

Applying this sensor on both cables of the power lines, we obtain the differential input of our system, as shown in Fig. 5a, which is equivalent to model the input voltage between the terminals of two capacitors depicted in the scheme of Fig. 5b.

3.6 Mathematical model

The problem consists in calculating two unknown variables (i.e., the capacitance C and the voltage V_{in}) from data acquired by the ADC. To do this, we use two equations,

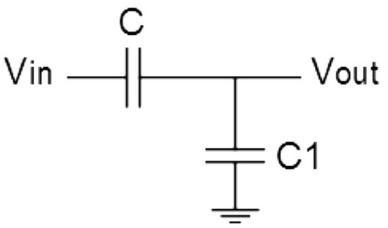

Fig. 6 The first of the two filters used to implement the mathematical two-equation system that models the problem

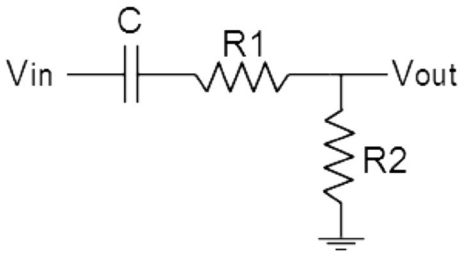

Fig. 7 The second filter used to implement the mathematical system

given by the transfer functions of the two analog filters implemented to realize the analog processing front end.

The first filter is shown in Fig. 6. It is an impedance voltage divider, made of two capacitances: the input unknown capacitance C and a capacitance C_1 of 6.8nF, whose optimal value has been estimated through simulations and verified with experiments, to discern even smaller values of the input voltage and not to exceed the microcontroller ADC conversion range.

The input–output relationship of this CC filter is:

$$V_{outCC} = \frac{C}{C + C_1} V_{in} \tag{2}$$

This is a real function, and the attenuation of V_{in} depends on the input capacitance C, without modifying its phase.

The second filter is shown in Fig. 7, and consists of a high-pass filter with a resistance voltage divider (R_1 of 1 GΩ, and R_2 of 3 MΩ) in series to the input capacitance. The resistance values are calculated with the aim of keeping the output signal in the available range and maximizing the dynamic, as well.

The transfer function of this CRR filter is:

$$H_{CRR}(s) = \frac{V_{outCRR}}{V_{in}} = \frac{sCR_2}{1 + sC(R_1 + R_2)} \tag{3}$$

The cut-off frequency of this filter is given by:

$$f_t = \frac{1}{2\pi C(R_1 + R_2)} \tag{4}$$

From the transfer function, the resulting module and phase of the frequency response of this filter are given by:

$$|H_{CRR}(j\omega)| = \frac{\omega CR_2}{\sqrt{1 + \omega^2 C^2 (R_1 + R_2)^2}} \tag{5}$$

$$\phi_{CRR} = \phi_{CRR}(\omega, C) \tag{6}$$

Starting from the phase ϕ_{CRR}, that is the phase shift corresponding to the delay between the V_{outCC} waveform (that is in phase with V_{in}) and the V_{outCRR} waveform (that is shifted of ϕ_{CRR} from Vin and, therefore, from V_{outCC}), we calculate the value of the input capacitance C by reversing (6), and then the waveform of V_{in}, by reversing (2).

3.7 The analog front end

A complete analog front end has been designed for the voltage measurement system. Each input channel is connected to both the CC filter and the CRR filter through a MCU-controlled switch, used to select the filter connected to the cable. Every filter output is decoupled from the downstream circuit by a buffer. Then we used an OPAMP in differential configuration to send a differential signal to the ADC. To avoid waste of energy when voltage measurement is not performed, all OPAMPs are turned off when not working, with a MCU-controlled pMOS which enables/disables their power supply. We also introduced a reference voltage (generated from the supply voltage) in the common mode node of filters and OPAMPs to bias their output voltages to positive values and therefore get the system to work correctly also in the negative semi-period of input signal.

3.8 Voltage measurement algorithm

The following steps summarize the algorithm designed to implement voltage measurement:

1. when the node wakes up from the sleep mode, it samples a period of V_{outCC} and then, after an exact multiple of signal periods from the beginning of sampling of V_{outCC}, samples a period of V_{outCRR};
2. measures the delay between V_{outCC} and V_{outCRR}, and converts this time in an angle (considering that a delay of a whole period corresponds to a phase shift of 360°), obtaining ϕ_{CRR};
3. knowing ϕ_{CRR}, calculates C from the reverse of the (6):
$$C = C(\omega, \phi_{CRR}) \tag{7}$$
4. knowing V_{outCC} waveform and C, calculates V_{in} waveform from the reverse of the (2):
$$V_{in} = \left(1 + \frac{C_1}{C}\right) V_{outCC} \tag{8}$$

3.9 Power features calculation

From the sample arrays of several periods of current signal and V_{in} signal, we can get the root mean square values for input current and voltage, using the formulas:

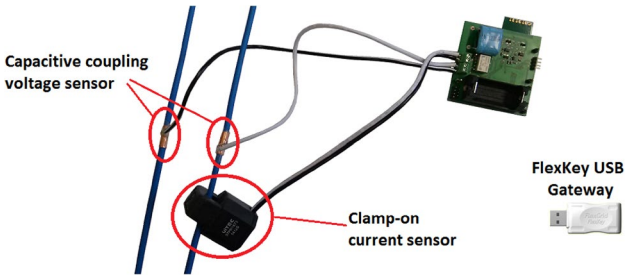

Fig. 8 Contact-less smart power meter prototype

$$V_{RMS} = \sqrt{\frac{1}{N}\sum_{k=0}^{N-1} v^2[k]} \tag{9}$$

$$I_{RMS} = \sqrt{\frac{1}{N}\sum_{k=0}^{N-1} i^2[k]} \tag{10}$$

Hence, we can calculate the apparent power |S| with the following:

$$|S| = V_{RMS} \cdot I_{RMS} \tag{11}$$

We can also calculate the active power P directly from the instantaneous powers p[k]:

$$P = \frac{1}{N}\sum_{k=0}^{N-1} p[k] = \frac{1}{N}\sum_{k=0}^{N-1} v[k]i[k] \tag{12}$$

As the active power P can be also written with the following:

$$P = V_{RMS} \cdot I_{RMS} \cdot PF \tag{13}$$

hence, we can calculate the power factor PF as:

$$PF = \frac{P}{|S|} \tag{14}$$

Finally, we can calculate the absolute value of the reactive power Q with the following:

$$Q = |S|\sqrt{1 - PF^2} \tag{15}$$

Figure 8 shows the prototype of the single-phase smart metering system described above.

4 Three-phase extension

A schematic view of the three-phase version of the proposed smart meter is shown in Fig. 9

The three-phase device is quite similar to the single-phase model described above, as can be noted in this figure. A current transformer is set to each of the three phase cables, and their outputs is used both for energy harvesting and for current measurement. A capacitive coupling voltage sensor is installed on each of the three phase cables and on the neutral cable, and, as shown in the following, the voltage measuring technique is the same of the single-phase version.

The only significant difference with the single-phase device is the external ADC used to sample simultaneously all the voltage and current channels: for this purpose, we used the 14-bit low-power Linear Technology LTC1408 ADC, which permits to sample simultaneously up to six

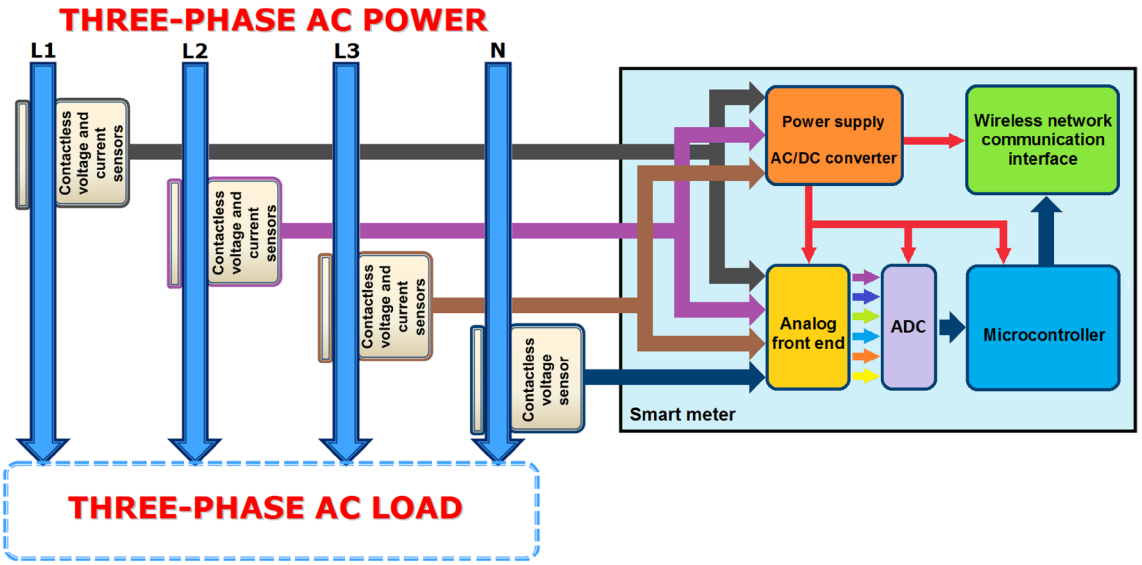

Fig. 9 Schematic view of the three-phase version of the smart meter, with the main blocks that compose it

differential inputs at a frequency of 600 ksps. Data is then sent to the MCU through the SPI protocol.

4.1 Current sensing and energy harvesting section

The current coming from each sensor is routed (with a latching-coil relay controlled by the MCU) either the energy harvesting system (that is shared for all the three lines and similar to the one presented in Sect. 3.3) or the current measurement circuit, where it is converted, with a resistance, to a proportional voltage, which is then sampled by a differential channel of the external ADC (simultaneously to the two other current channels and the three voltage channels), sent through SPI to the MCU, and finally elaborated by the 32-bit microcontroller.

An additional CT is used for the neutral-cable. This is used to assess the current with unbalanced three-phase loads, and since this current is supposed to be small, the Ct is not used for the energy harvesting sub-circuit.

4.2 Voltage sensing section

A schematic view of the voltage sensing section for all the three phases is shown in Fig. 10.

The signal coming from each voltage sensor is routed (using a MCU-controlled signal that drives all the relays) either to the CC filter shown in Fig. 6, or to the CRR filter shown in Fig. 7. The output of each filter is decoupled from downstream circuit with a buffer, then is selected with another relay (controlled by the same MCU signal). Then it is sampled by an external ADC with dual-end channels. Converted data is sent through SPI to the MCU, and finally elaborated by the 32-bit microcontroller using the algorithm described in Sect. 3.4.

When the CC filters are selected, each of the three phase lines is sampled by a differential channel of the external ADC using the CC filter output of the neutral line as the negative input, as shown in Fig. 11.

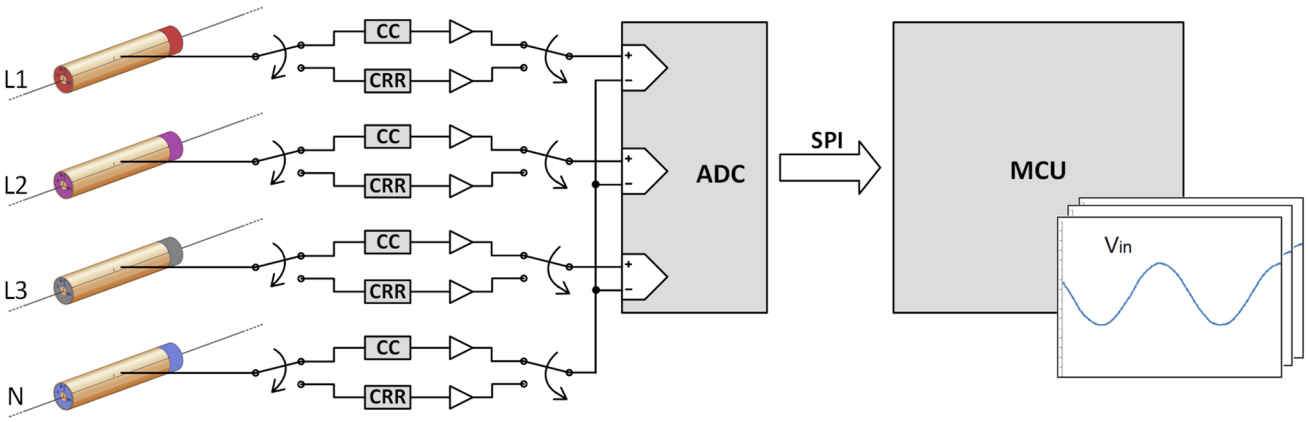

Fig. 10 Schematic view of the voltage sensing section for the three phases

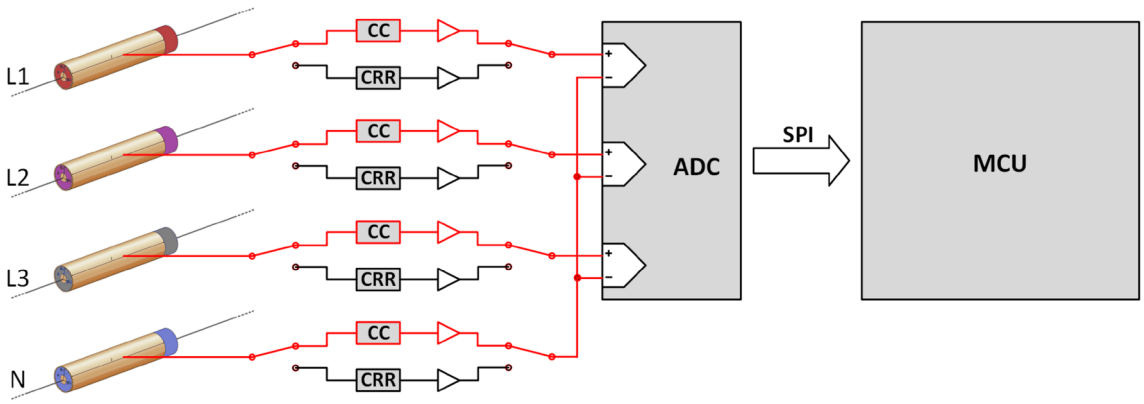

Fig. 11 Schematic view of the voltage sensing section with the CC filters selected

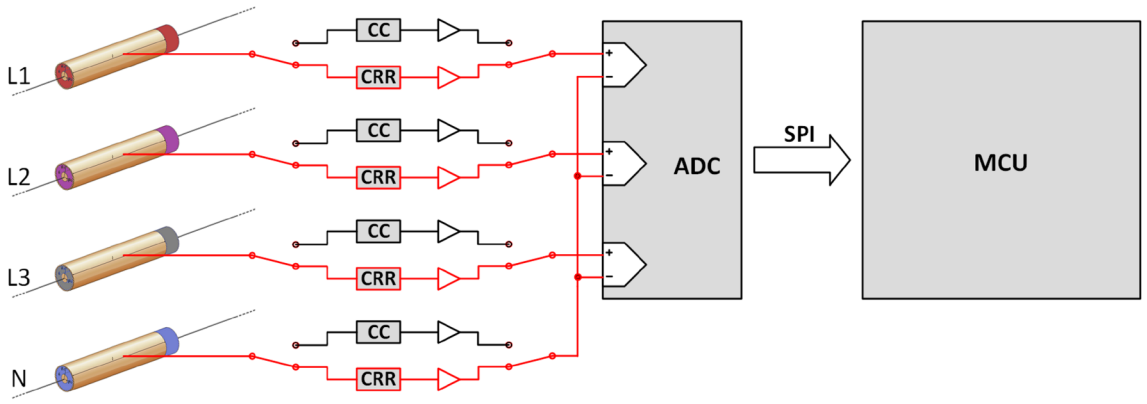

Fig. 12 Schematic view of the voltage sensing section with the CRR filters selected

The dual happens when the CRR filters are selected: each of the three phase lines are sampled by a differential channel of the external ADC using the CRR filter output of the neutral line as the negative input, as shown in Fig. 12.

This architecture permits to replicate easily the analog front-end presented in Sect. 3. The relays are latching coil type, which permits to perform a commutation using short pulses instead of delivering continues current to the coil. However, the output current of the MCU is not sufficient to commutate all the relays and thus we added a current buffer to the GPIO output. The switch losses are minimized due to the galvanic contact of the relay and, in the same time, they permit to transfer bipolar signals.

5 Experimental results

All tests were realized with the highest ADC sampling frequency for the JN5148 microcontroller, 100 kHz, and with a sleep time for the sensor node of 60 s. The cables used for the tests include all the main types of wires for domestic applications, from AWG3 (at which corresponds a C of 12pF) to AWG15 (at which corresponds a C of 8pF), and are listed in Table 1.

Results for power factor measurement, reported for three types of cables and with three measurements for each of four different electric loads, are shown in Table 1, in which they are compared with the values measured with an intrusive power meter. Measured values demonstrate the performance of the proposed non-intrusive measurement system in comparison to professional instruments (see Table 2).

As can be noted, PF values measured with the proposed non-intrusive smart meter has an error from the values measured with the intrusive power meter lower than 2 % and a deviation from the measured average value for a fixed load lower than 0.5 %.

Table 1 Properties of the types of cable for domestic applications used for the tests

Cable external section diameter (mm)	Cable internal section diameter (mm)	Capacitance (pF)
8.0	5.5	12
6.0	4.0	11
4.5	3.0	10
3.5	2.0	9
3.0	1.5	8
2.5	1.5	8

Results for voltage measurement are shown in Table 3, reported for the bigger (AWG3) and the smaller (AWG15) form factor cables and for three types of electric load, with the percentage error on the measured average value and the value measured with an intrusive power meter. The error for the voltage measurement is negligible too, in fact it is lower than 3 %, as reported in the Table.

6 Conclusions

In this paper we presented a wireless smart meter, compliant to IEEE 802.15.4 standard, which exploits a current transformer for contactless current measurement and an innovative contactless manner to measure the voltage waveform in a single-phase electrical line, and computes power consumption features. The device is therefore much safer and easy to install. The proposed system is also energetically self-sustainable, thanks to an energy harvesting module, which uses the same current sensor used for current measuring. The achieved accuracy is high, in fact the error for the electrical parameter measurements (i.e., current and voltage waveforms, power features) is lower than

Table 2 Results for PF measurement for three types of cables, compared with the intrusive power meter measurements

	PF measured with the non-intrusive smart meter	PF measured with the intrusive power meter	Error from the intrusive power meter (in %)	Deviation from non-intrusive smart meter average value (in %)
AWG3 cable				
Load 1	0.9981	1.000	0.19	0.05007
	0.9987	1.000	0.13	0.01001
	0.9990	1.000	0.10	0.04006
Load2	0.7721	0.780	1.01	0.25874
	0.7841	0.780	0.53	0.22480
	0.7856	0.780	0.72	0.03393
Load 3	0.6160	0.610	0.98	0.40750
	0.6106	0.610	0.10	0.47270
	0.6139	0.610	0.64	0.06520
Load4	0.4945	0.490	0.92	0.16152
	0.4939	0.490	0.80	0.28266
	0.4975	0.490	1.53	0.44418
AWG8 cable				
Load 1	0.9985	1.000	0.15	0.00668
	0.9982	1.000	0.18	0.02337
	0.9986	1.000	0.14	0.01669
Load 2	0.8019	0.800	0.24	0.05401
	0.8003	0.800	0.04	0.25343
	0.8048	0.800	0.60	0.30744
Load 3	0.6186	0.610	1.41	0.25390
	0.6169	0.610	1.13	0.02161
	0.6156	0.610	0.92	0.23229
Load 4	0.4789	0.470	1.89	0.22323
	0.4769	0.470	1.47	0.19533
	0.4777	0.470	1.64	0.23229
AWG15 cable				
Load 1	0.9974	1.000	0.26	0.01671
	0.9982	1.000	0.18	0.06349
	0.9971	1.000	0.29	0.04678
Load 2	0.7979	0.800	0.26	0.04176
	0.7978	0.800	0.28	0.05429
	0.7990	0.800	0.13	0.09605
Load 3	0.6526	0.650	0.40	0.23441
	0.6540	0.650	0.62	0.02038
	0.6558	0.650	0.89	0.25479
Load 4	0.4955	0.490	1.12	0.28844
	0.4979	0.490	1.61	0.19453
	0.4974	0.490	1.51	0.09391

Table 3 Results for voltage measurement for the bigger and the smaller type of cables, for three types of electric load, with the deviation from the average value and the percentage error from the value measured with the intrusive power meter

	AWG3 cable			AWG15 cable		
	Measured Vrms (V)	Deviation from average value (%)	Error from value measured with intrusive power meter (%)	Measured Vrms (V)	Deviation from average value (%)	Error from value measured with intrusive power meter (%)
Resistive load						
Load 1	230	1.91	2.37	221	2.39	1.96
Load 2	227	0.48	1.38	222	1.67	0.80
Load 3	229	1.20	1.65	221	2.39	1.96
Capacitive-resistive load						
Load 1	229	1.20	2.10	221	2.39	1.52
Load 2	227	0.48	0.93	222	1.67	1.24
Load 3	230	1.91	1.46	222	1.67	2.11
Inductive-resistive load						
Load 1	229	1.20	1.65	225	0.24	0.20
Load 2	230	1.91	1.91	227	0.48	0.48
Load 3	231	2.63	2.67	224	0.96	0.52

3 %. Hence, results are comparable to professional (and intrusive) measurement instruments, but at a cost that is dozens of times lower.

Acknowledgments The research contribution presented in this paper has been supported by a research Grant from Telecom Italia, by the project FLEXMETER (Grant no: 646568) funded by the EU H2020 Framework Programme, and by the ARTEMIS Innovation Pilot Project: ARROWHEAD (Grant no: 332987) funded by the ARTEMIS Joint Undertaking.

References

Ahmad S (2011) "Smart metering and home automation solutions for the next decade," in Proc. of the international conference on Emerging Trends in Networks and Computer Communications, (ETNCC 2011), Apr 22–24 2011, pp 200–204

Alahakoon D, Yu X (2016) Smart electricity meter data intelligence for future energy systems: a survey. IEEE Trans Ind Inform 12(1):425–436

Alimardani A, Therrien F, Atanackovic D, Jatskevich J, Vaahedi E (2015) Distribution system state estimation based on nonsynchronized smart meters. IEEE Trans Smart Grid 6(6):2919–2928

Amin SM, Wollenberg B (2005) Toward a smart grid: power delivery for the 21st century. IEEE Power Energy Magazine 3:34–41

Balsamo D, Porcarelli D, Brunelli D, Benini L (2013) "A new non-invasive voltage measurement method for wireless analysis of electrical parameters and power quality," IEEE

Borkowski D, Wetula A, Bien A (2015) Contactless measurement of substation busbars voltages and waveforms reconstruction using electric field sensors and artificial neural network. IEEE Trans Smart Grid 6(3):1560–1569

Campbell B, Dutta P (2014) "Gemini: a non-invasive, energy-harvesting true power meter," in Real-Time Systems Symposium (RTSS), 2014 IEEE (pp 324–333)

Chen Y, Hsu W, Cheng S, Cheng Y (2014) A power sensor tag with interference reduction for electricity monitoring of two-wire household appliances. IEEE Trans Industr Electron 61(4):2062–2070

Depuru S, Wang L, Devabhaktuni V, Gudi N (2011) "Smart meters for power grid, challenges, issues, advantages and status," Power Systems Conference and Exposition (PSCE), 2011 IEEE/PES

"Earth Overshoot Day." [Online]. Available: http://www.footprintnetwork.org/en/index.php/GFN/page/earth_overshoot_day

"Energy@home." [Online]. Available: http://www.energy-home.it

Kubo T, Furukawa T, Fukumoto H, Ohchi M (2009) "Numerical estimation of characteristics of voltage-current sensor of resin molded type for 22kv power distribution systems," in ICCAS-SICE, pp 5050–5054

Liang J, Ng SK, Kendall G, John WM, Cheng (2010) "Load signature study—part 2: disaggregation framework, simulation, and applications," Power Delivery, IEEE Transactions on, vol. 25, no. 2, pp 561–569

Liang J, Ng SK, Kendall G, Cheng JW (2010b) Load signature study—part 1: basic concept, structure, and methodology. IEEE Trans Power Deliv 25(2):551–560

Misti SN, Birkett M, Bell D, Penlington R (2014) "A new trimming approach for shunt resistors used in metering applications," Electronic Design (ICED), 2014 2nd International Conference on, vol., no., pp 94–99, 19–21

Mitra R, Kota R, Bandyopadhyay S, Arya V, Sullivan B, Mueller R, Storey H, Labut G (2015) Voltage Correlations in Smart Meter Data. Proceedings of the 21th ACM SIGKDD international conference on knowledge discovery and data mining (KDD '15). ACM, New York, pp 1999–2008

Porcarelli D, Balsamo D, Brunelli D, Paci G (2013) "Perpetual and lowcost power meter for monitoring residential and industrial appliances," in Design, Automation Test in Europe Conference Exhibition, pp 1155–1160

Quilumba FL, Wei-Jen Lee, Heng Huang, Wang DY, Szabados RL (2015) "Using smart meter data to improve the accuracy of intraday load forecasting considering customer behavior similarities," in Smart Grid, IEEE Transactions on, vol. 6, no. 2, pp 911–918

Ripka P (2010) "Electric current sensor: a review," Meas Sci Technol, vol. 21, no. 11, pp 112001-1–112001-23

Tsang K, Chan W (2011) Dual capacitive sensors for non-contact ac voltage measurement. Sens Actuators A 167(2):261–266

Villani C, Balsamo D, Brunelli D, Benini L (2015) "Ultra-low power sensor for autonomous non-invasive voltage measurement in IoT solutions for energy efficiency," in Proc. SPIE 9517, Smart Sensors, Actuators, and MEMS VII; and Cyber Physical Systems, 95172I

Waeresch D, Brandalik R, Wellssow WH, Jordan J, Bischler R, Schneider N (2015) "Linear state estimation in low voltage grids based on smart meter data," in PowerTech, 2015 IEEE Eindhoven, vol., no., pp1–6

Wu L, Wouters P, van Heesch E, Steennis E (2011) "On-site voltage measurement with capacitive sensors on high voltage systems", in PowerTech. IEEE Trondheim 2011:1–6

Xiao C (2003) "An overview of integratable current sensor technologies," in Conf. Rec. IEEE 38th IAS Annu. Meeting, Salt Lake City, UT, USA, vol. 2, pp 1251–1258

Ziegler S, Woodward RC, Iu HH, Borle LJ (2009) Electric current sensors: a review. IEEE Sensors J 9(4):354–376